# Pale Lager Clarification Using Novel Ceramic Hollow-Fiber Membranes and $CO_2$ Backflush Program

**Alessio Cimini, Mauro Moresi**

Department for Innovation in the Biological, Agrofood and Forestry Systems,

University of Tuscia, Via S. C. de Lellis, 01100 Viterbo, Italy

Key words: beer clarification; ceramic hollow-fiber membrane; crossflow microfiltration; crossflow velocity; permeation flux; rough pale lager; transmembrane pressure difference.

* To whom all correspondence should be addressed.

Tel. n°: +39-0761-357497;

fax n°: +39-0761-357498;

e-mail: mmoresi@unitus.it

**Abstract**

In this work, the crossflow microfiltration (CFMF) performance of a rough pale lager, produced in the industrial brewery Birra Peroni Srl (Rome, Italy), was assessed in a bench-top rig, equipped with a 0.8-μm ceramic hollow-fiber membrane module, to overcome the recognized inefficacy of back-flushing cleaning techniques in ceramic multi-channel monolithic modules. In total recycle CFMF trials, as the transmembrane pressure difference (TMP) was increased from 0.59 to 3.56 bar the quasi-steady state permeation flux (J*) tended to a limiting value increasing with the cross-flow velocity ($v_S$). To minimize the overall membrane surface to be installed for a prefixed permeate recovery, it was found to be expedient to operate at the aforementioned high cross-flow velocity and TMP of 3.56 bar, thus obtaining quite a high quasi-steady-state permeation flux (mean, μ: 173 L $m^{-2}$ $h^{-1}$; standard deviation, sd: 7 L $m^{-2}$ $h^{-1}$; number of observations, N: 12). The energy consumption per liter of permeate collected was found to be practically independent of the operating variables $v_S$ and TMP selected (μ: 55 W h $L^{-1}$; sd: 2 W h $L^{-1}$; N= 21). Yet, a permeate flux greater than 100 L $m^{-2}$ $h^{-1}$ was achieved on condition that TMP was greater than 2 bar and $v_S$ varied from 4 to 6 m $s^{-1}$. A few validation batch CFMF tests, carried out using pre-centrifuged, PVPP-stabilized, and cartridge-filtered rough pale lager at TMP = 3.56 bar, $v_S$ = 6 m $s^{-1}$ and 10 °C under a predefined $CO_2$ backwashing program, resulted in an average permeation flux (μ: 239 L $m^{-2}$ $h^{-1}$; sd: 24 L $m^{-2}$ $h^{-1}$;N: 2) by far greater than that (50-100 L $m^{-2}$ $h^{-1}$) claimed at 0-2 °C by the three CFMF processes commercially available. Finally, it was proved the easy transferability of the lager beer clarification and stabilization process, previously developed in a single-tube membrane module, to a ceramic hollow-fiber membrane module industrially upscalable.

## Introduction

The beer industry is potentially interested to replace conventional diatomaceous earth (DE) filters with crossflow microfiltration (CFMF) systems to get rid of the environmental and safety concerns connected with filter-aid handling and spent filter sludge disposal. Unfortunately, the average beer permeation flux through polyethersulphone hollow-fiber membrane modules is about a fifth of that (250-500 L $m^{-2} h^{-1}$) obtained with powder filters (Buttrick, 2007; Fillaudeau et al., 2006).

In beer CFMF the permeation flux is mainly controlled by the cake layer deposited onto the membrane surface (Cimini and Moresi, 2014). Thus, several hydrodynamic techniques (i.e., co-current mode; pulsating flow; periodic stop of the transmembrane pressure difference; periodic back-flush or back-shock process; generation of Dean or Taylor vortices; gas–liquid or liquid–solid flow; use of turbulence promoters, such as baffle channel or stamped membrane) have been studied by Blanpain et al. (1999), Fillaudeau et al. (2007), Gan et al. (1997), Kuiper et al. (2002), and Sondhi and Bhave, R. (2001) in order to enhance the CFMF performance.

To optimize the design of a back-flush regime, it is necessary to minimize permeate usage as back-flush medium so as to achieve pore clearance in the shortest time interval. Gan (2001) developed a multi-stage back-pulse routine capable of varying the $CO_2$ feed pressure, the duration of the pulse, the interval between the end of the pulse and opening of the permeate valve, as well as cycle frequency. These variables affected the membrane cleaning efficiency of the back-pulse, and the overall permeate loss. By selecting appropriately such variables, Gan (2001) was successful at improving the ten-hour average permeation flux to as much as 22 kg $m^{-2}$ $h^{-1,}$ this value being the

400% of that achieved during the cross-flow filtration formerly standardized (Gan et al., 1997).

In previous work (Cimini and Moresi, 2014), laboratory-made green beers were pre-centrifuged to minimize the fouling contribution of yeast cells and aggregates and reduce their initial haze level to 1.0-1.3 EBC unit, and then clarified to a final haze ≤ 0.5 EBC unit in a bench-top plant, equipped with a ceramic single-tube membrane module having nominal pore size of 0.8 μm under constant feed superficial velocity ($v_S$=6 m $s^{-1}$), transmembrane pressure difference (TMP=3-4 bar), temperature (T =10.0±0.5 °C), and periodic $CO_2$ back-flushing. In the circumstances, the average permeation flux ranged from 300 to 385 L $m^{-2}$ $h^{-1}$ thanks also to the efficacy of the $CO_2$ back-flushing program applied to the single-tube membrane module. Such a procedure was further tested on a rough pale lager produced in the industrial brewery Birra Peroni Srl (Rome, Italy), thus obtaining an average permeation flux of (252 ± 21) L $m^{-2}$ $h^{-1}$ (Cimini and Moresi, 2015). In addition, by stabilizing firstly pre-centrifuged beer with 0.5 g $L^{-1}$ of regenerable polyvinylpolypyrrolidone (PVPP) at 0 °C for 24 h , removing the sediment, pre-filtering the stabilized beer via a 2.7-μm cartridge to get rid of residual PVPP particles, and finally crossflow micro-filtering, it was possible not only to reduce the permeate chill haze to (0.31±0.06) EBC unit, but also to increase the average permeation flux to a value (337±1 L $m^{-2}$ $h^{-1}$) quite near to that achievable with conventional DE-filters (Buttrick, 2007).

The scaling-up of both operating conditions and back-flushing program from a ceramic single-tube membrane to a multi-channel monolithic module, such as for instance the Membralox® ceramic monolith type EP3740 (Pall Corporation, 2007), is generally hampered by the difficulty of assuring appropriate and constant permeate flow

rates throughout all the channels of the monolith. In fact, Doleček and Cakl (1998) showed that the contribution of some channels to the total permeation flux depended on either the ratio of skin layer to porous support permeability or the distance of a channel from the membrane outer surface. Thus, the cake layer deposited onto the membrane surface of the inner channels of the monolith may be poorly back-flushed by the local $CO_2$ flow rate, thus yielding permeation fluxes quite lower than those obtained previously in a ceramic single-tube membrane.

The aim of this work was to assess whether the aforementioned combination of operating conditions and $CO_2$ back-flushing program might succeed in clarifying pre-centrifuged rough pale lager using a novel ceramic hollow-fiber membrane module having the same nominal pore size of 0.8 μm while keeping both the permeate turbidity and average permeation flux practically unchanged.

## Materials and Methods

*Raw Materials*

The rough pale lager used here was produced by the industrial Birra Peroni Srl brewery (Rome, Italy). It was withdrawn from the maturation tanks and stored at 0.0±0.5 °C. Before CFMF testing, the rough lager samples were clarified using a laboratory centrifuge (Beckman mod. J2-21) at 6000 x *g* and ≤4 °C for 10 min, and then diluted with de-ionized water as recommended by the brewmaster to reach an ethanol content near to the commercial one (4.7 ± 0.1 % v/v).

*Equipment and experimental procedure*

Beer clarification was carried out using the bench-top CFMF plant, previously described (Cimini and Moresi, 2014). In this work, it was equipped with an $\alpha$-$Al_2O_3$ hollow-fiber InoCep® membrane module type MM04 (Hyflux Ltd, Singapore; http://www.hyfluxmembranes.com/inocep-ceramic-hollow-fibre-membrane.html). Such a module consisted of 40 hollow-fibers with an inside diameter ($d_{HF}$) of 3 mm, an overall length ($L_{HF}$) of 200 mm, an effective membrane surface area ($A_m$) of 0.04 $m^2$, as well as nominal pore size of 0.8 μm (type M800) and water permeability of 2,500 L $m^{-2}$ $h^{-1}$ $bar^{-1}$ at 25 °C. Fig. 1a shows the overall (a) and front (b) views of the membrane module used.

Pre-centrifuged lager was fed to the membrane module using a centrifugal pump type HMS (Lowara, Montecchio Maggiore, Italy) with the following characteristics: maximum volumetric flow rate, 4,200 L $h^{-1}$; head, 40 m of water; brake power, 0.45 kW.

Several hydraulic tests were carried out at 20 °C by varying TMP in the range of 0.5-4.0 bar, the main results of which being shown in Fig. 2. In particular, TMP was calculated as the average of the inlet and outlet pressures, minus permeate backpressure (Cheryan, 1998):

$$TMP = (P_{in} + P_{out})/2 - P_P \quad (1)$$

where $P_{in}$, $P_{out}$, and $P_P$ are the experimental pressures at the inlet, outlet, and permeate ports of the membrane module used.

Despite the asynchronous motor driving the centrifugal pump was piloted by means of a frequency inverter VF type Commander SK 0.75 k (Control Techniques, Powys, UK), the feed flow rate ranged from 400 to 2,340 L $h^{-1}$, this corresponding to a cross-flow velocity inside the membrane module ($v_S$) varying from 0.4 to 2.3 m $s^{-1}$. To apply the same operating crossflow velocity ($v_S$) of 6 m $s^{-1}$, previously used to pilot a 0.8-μm ceramic single-tube membrane module with an inside diameter ($d_T$) of 6 mm and a length of 0.5 m (Cimini and Moresi, 2014), the novel hollow-fiber membrane module should have the same open cross-sectional area (a) of the tubular one, this involving the following condition

$$a = n_{HF} (¼ \pi d_{HF}^2) = ¼ \pi (d_T)^2 \quad (2)$$

where $n_{HF}$ is the number of open hollow-fibers needed. Thus, it was necessary to seal 36 out of 40 hollow-fibers. This was carried out by applying a continuous bead of silicone adhesive (Silastic® E-RTV Silicone Rubber Kit, Dow Corning Co., Midland, MI, USA) over the inlet and outlet openings of such hollow-fibers, the resulting silicone plug (Fig. 1c) remaining flexible even after curing and resisting chemicals including water. For reuse, a simple removal of the cured product was needed. To avoid any leakage during

153 the operating conditions tested, all the silicone-sealed hollow fibers were covered by a
154 stainless steel disk, as shown in Fig. 1d.

155 To assess the effects of TMP and $v_S$ on the volumetric permeate flux, pre-
156 centrifuged rough lager samples were micro-filtered. The resulting retentate and
157 permeate were continuously recombined and re-circulated through the membrane
158 module under constant temperature (T=10.0±0.5 °C). Initially, TMP and $v_S$ were set at
159 about 1 bar and 1.5 m $s^{-1}$, respectively. As the quasi-steady state permeation flux ($J^*$)
160 had been approached for as long as 15 min, TMP was step-wisely augmented from
161 about (1 to 4) bar. Moreover, during any step TMP was kept constant, while the
162 crossflow velocity was in sequence increased from (1.5 to 2.0, 2.5, 4.0, and 6.0) m $s^{-1}$.

163 Two final batch validation tests were carried out using pre-centrifuged, and
164 PVPP-stabilized rough pale lager samples. In particular, the stabilization process was
165 carried out as reported previously (Cimini et al., 2014; Cimini and Moresi, 2015). More
166 specifically, four 1.5-L cylindro-conical tanks were filled with pre-centrifuged rough
167 lager. Then, an amount of 0.75 g of regenerable PVPP was added to start the
168 stabilization process under a constant temperature (0.0 ± 0.5 °C). After 24-h incubation,
169 the spent PVPP-polyphenol aggregates gone to the bottom of the tank were withdrawn.
170 Finer residual aggregates were removed by vacuum filtration through 2.7-μm Whatman
171 filters (cat. No. 1823 047). Final beer clarification was performed using the partitioned
172 hollow-fiber membrane module by using two different procedures.

173 Firstly, two batch CFMF tests were carried out using the same operating
174 conditions applied to a ceramic single-tube membrane module (TMP = 3.73 bar, $v_S$ = 6
175 m $s^{-1}$, T = 10.0±0.5 °C) in combination with the same $CO_2$ backflush program (Cimini
176 and Moresi, 2015). As the permeation flux ($J_v$) approached the quasi-steady state flux

(J*), the pressure in the retentate side was manually reduced to 1 bar and two electro-valves were automatically opened or closed using a programmable logic controller-based process (PLC) to adjust the pressure difference between the permeate and retentate sides at + 3 bar for 2 min (Cimini and Moresi, 2014). In this way, the $CO_2$ back-flushing cycles differed one from another not only in duration, but also in timing. The overall CFMF performance was determined by calculating the average permeation flux ($J_{v,av}$) as follows:

$$J_{v,av} = \frac{\int_0^{t_{max}} J_v(t)\, dt}{t_{max}} \qquad (3)$$

where $t_{max}$ is the end time of the batch test. The function $J_v(t)$ was numerically integrated using the Simpson's rule with a constant time increment of 1 min.

A second validation test was carried out in agreement with the operating procedure recommended by Hyflux Membrane Manufacturing (2010). More specifically, stabilized pale lager samples were submitted to batch CFMF under constant $v_S$ (1.5 m $s^{-1}$) and T (10.0±0.5 °C), while setting initially the feed input pressure ($P_{in}$) and TMP at 2 and 0.96 bar, respectively. As soon as $J_v$ had declined to the quasi-steady state flux (J*), TPM was step-wisely increased to 1.96, 2.92, and 3.84 bar by setting $P_{in}$ at 3, 4, and 5 bar, respectively. The overall performance of such a test was assessed by estimating $J_{v,av}$ using Eq. (3).

Membrane cleaning was performed as indicated by Gan et al. (1999). In details, the membrane module was initially rinsed with tap water. Then, it was filled with an aqueous solution of NaOH at 0.3 % (w/w), that was gradually heated up to 60 °C with a maximum heating rate of 4 °C $min^{-1}$. Such a solution was then enriched with 0.5 % (v/v) hydrogen peroxide (at a percentage strength of 12 % v/v), and kept re-circulating

through the membrane module at about 60 °C for not less than 15 min. Subsequently, the module was rinsed with fluent demineralized water at 60 °C for 15 min. Next, the demineralized water was laced with HCl till a content of 0.3 % (w/w), and kept re-circulating at about 60 °C for not less than 30 min. Final rinsing was performed using demineralized water, the temperature of which was progressively decreased from 60 to 20 °C. Such a cleaning procedure was generally sufficient to restore the initial hydraulic permeability of the membrane module; otherwise, it was repeated. Membrane cleaning was performed before any total recycle or validation test at time intervals ranging from 15 h to 3.0-3.6 h, respectively.

*Analytical Methods*

The main characteristics [i.e., pH (EBC method no. 9.35); density, ρ (no. 9.43.1); viscosity, η (no. 9.38); turbidity or haze, H at 20 and/or 0 °C (no. 9.29); color, C (no. 9.6); and total phenol, TP (no. 9.11), β-glucan, BG (no. 8.11.1), real extract, RE, and original extract, OE (no. 9.4), and ethanol, A (no. 9.2.1) contents] of the beer or permeate samples were determined in compliance with the European Brewing Convention (2010) by referring to the EBC methods reported between round brackets.

Despite the pale lager used here was industrially produced, the variability in the rough pale lager samples submitted to CFMF testing was probably due to a few inevitable differences in wort production, lautering, fermentation, and beer maturation.

*Statistical analysis of data*

Hydraulic tests were triplicated and repeated at different times, while pale lager clarification tests using the hollow-fiber membrane module were duplicated to assess

224 the error variance for the all the experimental campaign, as recommended by
225 Montgomery (2005). Generally, the average coefficient of variation in the estimated
226 permeation flux ($J_v$) within data population was of the order of 10%.

227 Finally, the main properties of centrifuged rough lager samples, as well as their
228 corresponding permeates, were measured at least three times, and their means used for
229 further analysis.

230

## Results and discussion

*Hydraulic tests for the novel ceramic hollow-fiber membrane module*

The membrane module used here consisted of 40 hollow-fibers with inside ($d_{HF}$) and outside diameters of 3 and 4 mm, and an overall length ($L_{HF}$) of 200 mm. Such a bundle of ceramic tubes was hold together by a glue that irregularly covered the external surface of any tube. Thus, the manufacturer claimed that the nominal effective surface area of the membrane module was equal to 0.04 $m^2$, this being quite smaller than the geometrical one ($= \pi\, d_{HF}\, L_{HF} = 0.075\ m^2$).

In the hydraulic tests, the experimental permeate mass flow rate ($Q_p$) is a linear function of the transmembrane pressure difference (TMP) applied, being not affected by the feed superficial velocity for the lack of concentration polarization (Cheryan, 1998), and can be expressed as follows:

$$Q_p = \alpha_W\, TMP \qquad (4)$$

with

$$\alpha_W = \rho_W\, L_W\, A_m \qquad (5)$$

where $\alpha$ is the specific water permeation rate, expressed in g $s^{-1}$ $bar^{-1}$, $L_W$ is the hydraulic permeability, commonly expressed in L $m^{-2}$ $s^{-1}$ $bar^{-1}$, $\rho_W$ the density of water (in g $L^{-1}$), and $A_m$ the effective membrane surface area (in $m^2$).

Fig. 2 shows $Q_p$ against TMP either for the membrane module as received (closed symbols) or after several subsequent hydraulic tests repeated over a time interval of 6 months (open symbols). In both cases, the analysis of variance for the linear model of $Q_p$-vs.-TMP, including or not the intercept, allowed the intercept to be neglected, being

254 statistically insignificant at the 95% confidence level. Thus, $Q_P$ was proportional to
255 TMP for $v_S$ varying from 0.5 to 1.5 m $s^{-1}$.

256 Table 1 shows the specific water permeation rate ($\alpha_W$) together with the
257 corresponding coefficient of determination ($r^2$) and number of observations (N), where
258 $\alpha_W$ was determined by using the least squares method. It can be noted a certain
259 reduction in the membrane permeability as due to irreversible fouling. When the module
260 was partitioned by sealing 36 out of 40 tubes to assure as high feed crossflow velocities
261 as 4-6 m $s^{-1}$ in each hollow-fiber using the centrifugal pump available, the hydraulic test
262 allowed the specific water permeation rate for the partitioned module ($\alpha_{Wp}$) to be
263 determined (Fig. 2). Thus, the effective membrane surface area of the partitioned
264 module ($A_{mp}$) was empirically estimated by assuming that all the hollow-fibers of the
265 membrane module had the same hydraulic permeability:

266 $$A_{mp} = A_m \frac{\alpha_{Wp}}{\alpha_W} = 0.0071 \text{ m}^2$$

267 Such an effective membrane surface area was used to derive the volumetric
268 permeation flux ($J_v$) from the instantaneous permeate mass rate ($Q_p$) as

269 $$J_v = \frac{Q_P}{\rho_P A_{mp}} \qquad (6)$$

270 where $\rho_P$ is the permeate density.

271 By referring to Table 1, during these CFMF trials the experimental water
272 permeability of the ceramic hollow fiber membrane module at 20 °C was equal to (1701
273 ± 54) L $m^{-2}$ $h^{-1}$ $bar^{-1}$.

274

275

*Effect of TMP and $v_S$ on permeation flux*

Table 2 shows the main characteristics of the pale lager used in this work, as collected from the brewery maturation tank (RB) and as PVPP-stabilized and diluted with water as recommended by the Peroni brewmaster (F).

To verify the effects of TMP and $v_S$ on $J_v$, the pre-centrifuged rough lager samples having turbidity of ~1.16 EBC unit were micro-filtered, and the resulting retentate and permeate continuously recombined and re-circulated through the membrane module under constant temperature (10.0±0.5 °C) by setting initially TMP and $v_S$ at about 1 bar and 1.5 m $s^{-1}$, respectively. As the quasi-steady state permeation flux ($J^*$) had been approached for circa 15 min, the crossflow velocity was sequentially raised from 1.5 to 6.0 m $s^{-1}$. Such a procedure was then repeated by increasing TMP in sequence from about 1 to 4 bar, while resetting $v_S$ at 1.5 m $s^{-1}$.

To mark better the shear effect of $v_S$, the instantaneous permeation flux ($J_v$) was used to estimate the corresponding overall membrane resistance ($R_T$), as derived from Darcy's law:

$$J_v = \frac{TMP}{\eta_P R_T} \quad (7)$$

with

$$R_T = R_m + R_{irr} + R_{rev} \quad (8)$$

where $\eta_P$ is the permeate dynamic viscosity, and $R_T$, $R_m$, $R_{irr}$, and $R_{rev}$ are the overall membrane resistance, intrinsic membrane resistance, and resistances of the irreversible and reversible fouling layers, respectively. In particular, $R_{rev}$ includes concentration polarization and deposition of solids on the membrane surface (stationary cake layer), while $R_{irr}$ is due to interaction of the membrane with the particles and aggregates in the

feed stream and comprises of the blocking of the pores entrance and internal fouling inside the pores.

As shown in Fig. 3, during any TMP step of the total recycle CFMF test $R_T$ tended to increase with time (t) till reaching a quasi-steady state value ($R_T^*$). As $v_S$ was increased under constant TMP, $R_T$ displayed a quick decrease and generally tended to a smaller $R_T^*$ value. As TMP underwent a further step increase, $v_S$ was newly reduced to 1.5 m $s^{-1}$. The aforementioned $R_T$ trend was generally reproduced in all the subsequent steps, the ratio between the corresponding quasi-steady state overall membrane resistance ($R_T^*$) and intrinsic membrane one [$R_m = (1.62 \pm 0.03) \times 10^{11}$ $m^{-1}$] being by far greater than unity. Moreover, the minimum $R_T^*$ values resulted to be associated to $v_S$ = 6 m $s^{-1}$. Thus, at TMP=3.56 bar the limiting flux ($J^*$) resulted to be equal to (173 ± 7) L $m^{-2}$ $h^{-1}$ (Table 3).

Several studies have so far dealt with fluid dynamics in a porous tube under laminar (Vassilieff, 1994; Munson-McGee, 2002) and/or turbulent conditions (Mellis et al., 1993). In particular, the pressure drop along the porous tube length was found to be approximately parabolic in the laminar regime (Munson-McGee, 2002). By referring to the main conclusions by Mellis et al. (1993), the pressure drop along a porous tube depends on axial flow rate and wall suction, such variables depending on the axial feed ($Re_F$) and wall ($Re_W$) Reynolds numbers, respectively:

$$Re_F = \rho_R v_S d_{HF}/\eta_R \quad (9)$$

$$Re_W = \tfrac{1}{2} \rho_R v_W d_{HF}/\eta_R \quad (10)$$

where $v_W$ is the average wall velocity, this coinciding with the quasi-steady state permeation flux (J*), expressed in m $s^{-1}$.

According to Mellis et al. (1993), either at very low values of axial flow ($Re_F$<1,000) and wall suction ($Re_W$<0.25) or for $Re_F$>20,000 and $Re_W$ ranging from 0 to 1.25, the axial pressure drop was found to be minimally affected by wall suction and practically coincided with that estimated via the Darcy equation for a solid wall tube (Toledo, 2007):

$$\Delta P_D = 2\, f\, \rho_R\, (v_S)^2\, L_{HF}/d_{HF} \qquad (11)$$

where in this specific case $\Delta P_D$ is the pressure loss due to friction along the bundle of hollow fibers of given length $L_{HF}$, and f the Fanning friction factor.

As shown in Table 3, the wall Reynolds number ($Re_W$) ranged from 0.009 to 0.051, this ensuring the minimal effect of wall suction on the axial pressure drop both in the laminar and turbulent conditions (Mellis et al., 1993).

In this work, the Fanning friction factor (f) for laminar or turbulent flow in smooth circular pipes was estimated as follows (Toledo, 2007):

$$f = \begin{cases} 16/Re & \text{for } Re \le 2{,}100 \qquad (12) \\ 0.193\, Re^{-0.35} & \text{for } 3\times10^3 < Re < 10^4 \qquad (13) \\ 0.048\, Re^{-0.20} & \text{for } 10^4 < Re < 10^6 \qquad (14) \end{cases}$$

The feasibility of calculating the Fanning friction factor using the smooth-tube model, even when the hollow-fibers present a non-smooth surface in consequence of the progressive deposition of particles, was checked by referring to the measurements carried out by Pal et al. (2008), and Yazdanshenas et al. (2010). In particular, in the case of the ultrafiltration of simulated fruit juices consisting of pectin and sucrose using an organic polyphenylene ethersulfone membrane with a molecular mass cut-off of 30 kDa, the thickness of the cake thickness ranged from 10 to 16 μm, while J* varied from 9 to 33 L $m^{-2}$ $h^{-1}$ (Pal et al., 2008). A quasi-steady state permeation flux (J*) of about 10

346 L $m^{-2}$ $h^{-1}$ was achieved during the crossflow microfiltration of a rough non-alcoholic
347 beer with quite a high haze at 20 °C (42.5 EBC unit) across a ceramic tubular membrane
348 module with pore size of 0.45 μm, this being associated to the formation of a cake layer
349 of 30-40 μm (Yazdanshenas et al., 2010). In the CFMF tests performed here, the rough
350 beer was pre-centrifuged, PVPP-stabilized and cartridge-filtered, this making the rough
351 beer haze at 20 °C quite low (1.16±0.02 EBC unit), as shown in Table 2.

352 By assuming J* as inversely proportional to the thickness of the cake layer, in this
353 work the fouling layer should have varied from 13 to 2 μm for $v_S$ increasing from 1.5 to
354 6 m $s^{-1}$. In the circumstances, by assuming that the roughness (ε) of each hollow-fiber is
355 determined by the particles deposited, the relative roughness of the hollow fibers, that is
356 the ratio of their roughness to inner diameter (3 mm), would range from $6.7x10^{-4}$ to 4.3x
357 $10^{-3}$. By resorting to the Haaland equation (1983), that allows explicit calculation of the
358 fiction factor (f) in quite good agreement with that estimated via the Colebrook equation
359 (1938-39) when the Reynolds number and relative roughness are specified:

360 $$\frac{1}{\sqrt{f}} = -3.6\log_{10}[\frac{6.9}{Re} + (\frac{\varepsilon/d_{HF}}{3.7})^{10/9}] \quad (15)$$

361 it was possible to assess that the relative errors of the solutions of Eq.s (15) and (13) or
362 (14) for Re ranging from 3,000 to $10^4$ or 13,000 varied from -5 to +18%, this making
363 the Darcy friction factor estimated from Eq. (13) or (14) accurate enough owing to the
364 large uncertainties in the Darcy friction factor in such flow regimes (Haaland, 1983).

365 As shown in Table 3, the estimated pressure drop ($\Delta P_D$) was roughly the half of
366 the experimental one ($\Delta P_{exp}$), this being estimated as the difference between the
367 pressures analogically measured by the manometers located on the opposite ends of the
368 membrane module. It is worth noting that $\Delta P_D$ did not account for the so called minor

losses due to a few pipe fittings, such as the section enlargement to connect the 19.3-mm pipe to the 34-mm membrane housing, the section contraction to feed the hollow-fiber bundle, the section enlargement as the retentate flows out of the hollow-fiber bundle, and the final restriction encountered by the retentate flowing out of the membrane module. Among the methods generally used to account for the flow losses from friction in pipe fittings, contraction, or enlargement, those referring to the equivalent length ($L_e$) or resistance coefficient (K) of any pipe fitting, that is the length of pipe of the same size as the fitting or the number of velocity head terms ($\frac{1}{2} v_S^2/g$) that would give rise to the same pressure drop as the fitting, resulted in estimated minor losses (Anon, 2012; Crane, 1965) by far greater than those experimentally assessed by subtracting $\Delta P_D$ from $\Delta P_{exp}$. Altogether, the largest contribution to the overall minor losses was due to the sudden contraction from the housing tube to the bundle of four 3-mm hollow-fibers.

Fig. 4 shows the combined effect of $v_S$ and TMP on the quasi-steady state permeation flux J*. By operating at low $v_S$ values, such as 1.5-2 m $s^{-1}$, J* tended to be independent of TMP at TMP values just greater than 0.6 bar. As $v_S$ was increased from 2.5 to 4 m $s^{-1}$, the validity of the Darcy model extended up to TMP values of the order of 2 bar. Generally, the asymptotic J*.vs.-TMP relationship is attributed to the concentration polarization effect (Cheryan, 1998). In fact, any increase in TMP results in a thicker or denser cake layer deposited over the membrane surface that increases the overall filter resistance and thus limits the permeation flux to the so-called limiting flux. Such a phenomenon, known as concentration polarization, is inherent to all crossflow filtration processes for the membrane has different permeability for the various components of the solution or suspension (Cheryan, 1998). The lower the crossflow

velocity, the lower the limiting flux becomes. From Fig. 4, it can be noted that at $v_S$=6 m $s^{-1}$ J* was proportional to TMP for TMP < 4 bar. In fact, the analysis of variance for the linear model of J*-vs.-TMP, including or not the intercept, allowed the intercept to be neglected, being statistically insignificant at the 95% confidence level. Thus, J* was predicted via the following least squares regression equation:

$$J^* = (50.5 \pm 2.8)\ TMP \qquad (r^2 = 0.982) \qquad (16)$$

where the lager permeability for the ceramic hollow-fiber membrane module was about the 3% of the water permeability at 20 °C, previously assessed. The continuous line plotted in Fig. 4 illustrates the estimated J* values, while the broken lines refer to loci of the upper and lower confidence limits at the 95% confidence level.

For all the operating conditions tested, Table 3 also lists the theoretical pump power ($N_P$) needed to compress the rough lager feed ($Q_F$) from the storage tank kept at atmospheric pressure ($P_{atm}$) to the pressure ($P_{in}$) registered by the gauge placed at the inlet port of the membrane module. Therefore, the total dynamic head ($H_P$) of the centrifugal pump had to account for the differences in pressure, liquid elevation and velocity between the source and destination, as well as for the pipe and pipe fitting friction losses and the pressure drop through the instrumentation and other items in the flow path of the liquid. In the bench-top plant used here, the static head difference between the rough beer tank and membrane module was regarded as negligible, the beer velocity head at the top level of the storage tank practically nil owing to the total recycle tests performed, while the pressure drop over the pipe fittings connecting the storage tank to the centrifugal pump and the latter to the membrane module was, by rule of thumb, assumed as one fifth of the experimental pressure drop across the membrane

module itself. Thus, the theoretical power absorbed by the beer was evaluated as follows:

$$N_P = g\,\rho_F\,Q_F\,H_P \quad (17)$$

with

$$H_P = \tfrac{1}{2}\,v_s^2/g + (P_{in} - P_{atm} + \Delta P_{exp}/5)/(\rho_F\,g) \quad (18)$$

$$Q_F = Q_P + Q_R \quad (19)$$

$$Q_P = J^* A_m \quad (20)$$

$$Q_R = a\,v_S \quad (21)$$

where $Q_F$, $Q_P$ and $Q_R$ are the feed, permeate and retentate volumetric flow rates, and a is the overall cross section of the membrane module, as defined by Eq. (2).

As shown in Fig. 5, whatever the cross-flow velocity and TMP applied, $N_P$ appeared to be proportional to J*:

$$N_P = (0.39 \pm 0.02)\,J^* \qquad (r^2 = 0.962) \quad (22)$$

In fact, the analysis of variance for the linear model of NP-vs.-J*, including or not the intercept, allowed the intercept to be neglected for the following reasons: i) the intercept exhibited a negative value, statistically significant at the probability level of 0.024, but devoid of any physical meaning; ii) the coefficient of determination of Eq. (22) was greater than that pertaining to the empirical model including the intercept ($r^2$=0.907). The continuous line in Fig. 5 shows the $N_P$ values estimated using Eq. (22), while the broken lines refer to loci of the upper and lower confidence limits at the 95% confidence level.

Thus, despite a certain scattering of data, the energy consumption per unit liter of permeate recovered was practically constant (μ: 55 W h $L^{-1}$; sd: 2 W h $L^{-1}$; N= 21). Of course, such a figure did not include the power transferred from the electric motor to the

440 shaft of the centrifugal pump and from the blades to the lager to be clarified, this
441 depending on their corresponding efficiencies. Nevertheless, not all combinations of the
442 operating variables $v_S$ and TMP allowed a permeate flux greater than 100 L $m^{-2}$ $h^{-1}$ to be
443 assured. As shown in Fig. 4, such a CFMF performance might be achieved at TMP > 2
444 bar and $v_S$ of 4-6 m $s^{-1}$.
445

*Validation testing*

The effectiveness of the CFMF operating conditions yielding the higher value of the quasi-steady state permeation flux (173 ± 7) L $m^{-2}$ $h^{-1}$, that is TMP = 3.56 bar and $v_S$ = 6 m $s^{-1}$ (Table 3), was further established using pre-centrifuged, PVPP-stabilized and 2.7-µm pre-filtered rough pale lager together with the $CO_2$ backwashing program previously set up (Cimini and Moresi, 2014). The main characteristics of the rough pale lager sample (F) were listed in Table 2.

Contrary, to previous tests carried out on a pure malt beer containing as much as 140-250 mg $L^{-1}$ of β-glucans (Cimini et al., 2014), in this work no enzymatic depolymerization pretreatment was performed, the β-glucan content of the rough pale lager used being as small as (9±2) mg $L^{-1}$ (Table 2). Moreover, the 24-h PVPP-stabilization allowed the original total phenol content (152±5 mg $L^{-1}$) to be reduced to (89±2 mg $L^{-1}$).

Fig. 6 shows the time course of the experimental permeation flux ($J_v$: open symbols), when using the aforementioned $CO_2$ backwashing program. In the circumstances, the min-max variation in the quasi-steady state (J*) ranged from 152 to 200 L $m^{-2}$ $h^{-1}$ (µ=175 L $m^{-2}$ $h^{-1}$; sd=20 L $m^{-2}$ $h^{-1}$; N=19). Thanks to the periodic $CO_2$ back-flushing, the average permeation flux ($J_{v,av}$) improved to 239 L $m^{-2}$ $h^{-1}$ (sd=24 L $m^{-2}$ $h^{-1}$; N=2), as calculated using Eq. (3). Moreover, the beer permeate collected during these trials exhibited an average haze at (20 and 0) °C of (0.21±0.01) or (0.44±0.06) EBC unit, respectively. Thus, the permeated beer fulfilled the European Brewery Convention specification (2010) for a clear, bright beer (<0.6 EBC unit).

Fig. 6 also compares the typical time course of $J_v$ (closed symbols) for a similar pale lager sample previously submitted to batch CFMF through a 0.8-µm ceramic

single-tube membrane module under practically the same operating conditions (i.e., TMP ≈ 3.73 bar, $v_S$ = 6 m $s^{-1}$, T = 10.0±0.5 °C, and periodic $CO_2$ back-flushing), as extracted from Cimini and Moresi (2015). In that case, the mean values of $J^*$ and $J_{v,av}$ resulted to be equal to (138±8) and (337±1) L $m^{-2}$ $h^{-1}$, respectively (Cimini and Moresi, 2015).

Despite the average permeation flux obtained was just the 71% of that achieved with the single-tube module, the CFMF performance of the hollow-fiber membrane module tested here was on the whole by far greater than that (80-100 L $m^{-2}$ $h^{-1}$) claimed at (0-2) °C by the three CFMF processes commercially available (i.e., the Norit process filtering rough beer, previously sedimented under refrigeration, across 0.45-μm polyethersulfone hollow-fiber modules; and the Pall or Alfa Laval process filtering pre-centrifuged rough beer through 0.65-μm polyethersulfone hollow-fiber or flat-sheet membrane modules, respectively) (Buttrick, 2007). Moreover, filtering rough beer at 0-2 °C was found to be useless provided that the CFMF unit had been fed with pre-centrifuged, PVPP-stabilized, and cartridge-filtered rough beer (Cimini and Moresi, 2015).

Moreover, since the effectiveness of $CO_2$ back-flushing previously assessed in a single-tube module (Cimini and Moresi, 2014, 2015) is highly likely irreproducible in a multi-channel one (Doleček and Cakl, 1998), the use of such a novel hollow-fiber membrane module appeared to be the only way to transfer the lager beer clarification and stabilization process previously developed (Cimini and Moresi, 2015) from a bench-top rig to an industrial-scale plant.

To assess further the efficacy of the above operating procedure, another validation test was performed to simulate the procedure generally applied to counterbalance

494 typical flux decay during the operation of industrial dead-end or crossflow filters, this
495 involving a progressive or a step by step increase in TMP while keeping the crossflow
496 velocity constant (Noordman et al., 2001; Hyflux Membrane Manufacturing, 2010).

497 Fig. 7 shows the time course of the experimental permeation flux ($J_v$), as observed
498 when setting $v_S$ at 1.5 m $s^{-1}$ and fixing the initial TMP at 0.96 bar. As soon as the
499 permeation flux had reached the quasi-steady state permeation flux, the pressure ($P_{in}$) at
500 the input port of the membrane module was increased of about +1 bar. Such a procedure
501 was continued till a final $P_{in}$ value of 5 bar. Despite a sudden increase in $J_v$ had been
502 detected immediately after any step increase in the feed input pressure, $J_v$ tended to
503 decline with time to J*. Altogether, the mean values, standard deviations and numbers
504 of observations of J* and $J_{v,av}$ resulted to be equal to ($\mu$=42 L $m^{-2}$ $h^{-1}$; sd=8 L $m^{-2}$ $h^{-1}$;
505 N=35) and ($\mu$=64 L $m^{-2}$ $h^{-1}$; sd=7 L $m^{-2}$ $h^{-1}$; N=2).

506 It can be noted that the average permeation flux of the last validation test was
507 fully in line with that claimed by Hyflux Membrane Manufacturing (2010) when setting
508 $v_S$= 2 m $s^{-1}$ and increasing TMP step by step from (1.7 to 5.7) bar. Moreover, it was
509 possible to confirm the indifference of J* to $v_S$ and TMP in the ranges of 1.5-2 m $s^{-1}$ and
510 2-4 bar, respectively, as shown in Fig. 4.

511 By comparing the overall performances of the validation tests shown in Fig.s 6
512 and 7, the procedure involving the operation at $v_S$= 6 m $s^{-1}$ and TMP=3.56 bar resulted
513 to be the most expedient for the following reasons: (i) the average permeation flux was
514 about 4 times greater than that suggested by the hollow-fiber membrane module
515 manufacture, this reducing the depreciation and maintenance costs of the CFMF unit;
516 (ii) the theoretical electric energy consumed per liter of beer permeated collected was
517 practically constant, as shown by Fig. 5.
518

## Conclusions

The lager beer clarification and stabilization process previously developed using a 0.8-μm ceramic single-tube membrane module was successfully tested in the same bench-top rig equipped with a 0.8-μm ceramic four hollow-fiber membrane module to overcome the recognized inefficacy of back-flushing cleaning techniques in ceramic multi-channel monolithic modules.

In total recycle CFMF trials, that were used to simulate pale lager clarification in the continuous mode, the quasi-steady state permeation flux (J*) exhibited the typical phenomenon of concentration polarization with a limiting flux increasing with the cross-flow velocity ($v_S$). Particularly, at $v_S$ = 6 m $s^{-1}$ and TMP in the range of 0.59-3.56 bar J* was proportional to TMP, yielding a pale lager permeability as small as the 3% of the water permeability at 20 °C. By relating the theoretical pump power ($N_P$) needed to feed appropriately the membrane module to the corresponding quasi-steady state permeation flux, an average electric energy consumption of (55±2) W h per unit liter of permeate collected was assessed, this value being practically independent of the operating variables $v_S$ and TMP selected. Yet, a permeate flux greater than 100 L $m^{-2}$ $h^{-1}$ was achieved provided that TMP was greater than 2 bar and $v_S$ varied from 4 to 6 m $s^{-1}$.

A final validation batch CFMF test was carried out using pre-centrifuged, PVPP-stabilized, and cartridge-filtered rough pale lager by setting TMP to 3.56 bar and $v_S$ to 6 m $s^{-1}$ under predefined $CO_2$ backwashing program, thus obtaining an average permeation flux of (239±24) L $m^{-2}$ $h^{-1}$ by far greater than that claimed by the three CFMF processes commercially available.

Finally, such operating procedure was found to be even more expedient than that suggested by the ceramic hollow-fiber membrane module manufacturer. In fact, the

543 operation suggested by the membrane manufacture (i.e., $v_S$=2 m $s^{-1}$ under a progressive
544 increase in TMP from about 1.7 to 5.7 bar) resulted in an average permeation flux about
545 four times smaller than that achieved with the alternative procedure examined in this
546 work.
547
548
549 ***Acknowledgements***
550 This research was supported by the Italian Ministry of Instruction, University and
551 Research, special grant PRIN 2010-2011 - prot. 2010ST3AMX_003.
552

**Nomenclature**

| | | |
|---|---|---|
| a | Cross-sectional area of the hollow-fiber membrane module, as defined by Eq. (2) [$m^2$] |
| A | Alcohol content of beer [% v/v] |
| $A_m$ | Effective membrane surface area [$m^2$] |
| BG | β-glucan content of beer [mg $L^{-1}$] |
| C | Beer color [EBC unit] |
| CFMF | Crossflow microfiltration |
| $d_{HF}$ | Inside diameter of each ceramic hollow-fiber [m] |
| $d_T$ | Inside diameter of the tubular membrane module [m] |
| DE | Diatomaceous earth |
| f | Fanning friction factor [dimensionless] |
| H | Beer turbidity [EBC unit] |
| $H_P$ | Total dynamic head of the centrifugal pump [m] |
| $J^*$ | Quasi steady-state permeation flux [L $m^{-2}$ $h^{-1}$] |
| $J_v$ | Instantaneous volumetric permeation flux [L $m^{-2}$ $h^{-1}$] |
| $J_{v,av}$ | Average volumetric permeation flux, as defined by Eq. (3) [L $m^{-2}$ $h^{-1}$] |
| K | Resistance coefficient of any pipe fitting [dimensionless] |
| $L_e$ | Equivalent length of any pipe fitting [m] |
| $L_{HF}$ | Length of each ceramic hollow-fiber [m] |
| $L_W$ | Hydraulic permeability [L $m^{-2}$ $h^{-1}$ $bar^{-1}$] |
| $n_{HF}$ | Number of open hollow-fibers [dimensionless] |
| N | Number of observations [dimensionless] |
| $N_P$ | Theoretical pump power [W] |

| | | |
|---|---|---|
| OE | Beer original extract [°Plato] |
| $P_{atm}$ | Atmospheric pressure [Pa] |
| $P_{in}$ | Pressure at the inlet port of the membrane module [Pa] |
| $P_{out}$ | Pressure at the outlet port of the membrane module [Pa] |
| $P_P$ | Pressure at the permeate port of the membrane module used |
| PVPP | Polyvinyl-polypyrrolidone |
| $Q_F$ | Feed volumetric flow rate [$m^3$ $s^{-1}$] |
| $Q_p$ | Permeate mass flow rate [g $s^{-1}$] |
| $Q_P$ | Permeate volumetric flow rate [$m^3$ $s^{-1}$] |
| $Q_R$ | Retentate volumetric flow rate [$m^3$ $s^{-1}$] |
| $r^2$ | Coefficient of determination |
| RB | Rough beer |
| RE | Beer real extract [°Plato] |
| $Re_F$ | axial feed Reynolds number, as defined by Eq. (9) [dimensionless] |
| $Re_W$ | wall Reynolds numbers, as defined by Eq. (10) [dimensionless] |
| $R_{irr}$ | Irreversible fouling resistance [$m^{-1}$] |
| $R_m$ | Intrinsic membrane resistance [$m^{-1}$] |
| $R_{rev}$ | Reversible fouling resistance [$m^{-1}$] |
| $R_T$ | Overall membrane resistance [$m^{-1}$] |
| $R_T^*$ | Quasi-steady state overall membrane resistance [$m^{-1}$] |
| T | Process temperature [°C] |
| sd | Standard deviation |
| t | Process time [s or h] |
| $t_{max}$ | End time of any rough beer permeation test [h] |

| | | |
|---|---|---|
| TMP | Transmembrane pressure difference [bar] |
| TP | Total phenolic content [mg $L^{-1}$] |
| $v_S$ | Crossflow velocity [m $s^{-1}$] |
| $v_W$ | average wall velocity [m $s^{-1}$] |

***Greek Symbols***

| | |
|---|---|
| $\Delta P_D$ | Pressure drop due to friction in smooth circular pipes [Pa] |
| $\alpha_W$ | Specific water permeation rate [g $s^{-1}$ $bar^{-1}$] |
| $\varepsilon$ | Hollow-fiber roughness (mm) |
| $\Delta P_{teo}$ | Theoretical pressure drop due to friction in smooth circular pipes [Pa] |
| $\eta$ | Dynamic viscosity [mPa s] |
| $\mu$ | Mean value |
| $\rho$ | density [kg $m^{-3}$] |

***Subscripts***

| | |
|---|---|
| av | average |
| exp | experimental |
| F | referred to beer feed |
| p | related to the partitioned hollow-fiber membrane module |
| P | referred to permeate |
| R | referred to retentate |
| W | referred to water |

## References


Anon (2012) Pressure drop in pipe fittings and valves. A discussion of the equivalent length ($L_e/D$), resistance coefficient (K) and valve flow coefficient ($C_v$) methods. Harvey Wilson - Katmar Software (available at http://www.katmarsoftware.com/articles/pipe-fitting-pressure-drop.htm, last checked on May, 5th, 2015).

Blanpain-Avet, P., Doubrovine, N., Lafforgue, C., & Lalande, M. (1999). The effect of oscillatory flow on cross-flow microfiltration of beer in a tubular mineral membrane system - membrane fouling resistance decrease and energetic considerations. *Journal of Membrane Science,* 152, 151-174.

Buttrick, P. (2007). Filtration – the facts. *The Brewer & Distiller International*, 3(1), 12-19.

Cheryan, M. (1998). *Ultrafiltration and Microfiltration Handbook*. Technomic Publ. Co., Lancaster, pp. 13-29, 120-130.

Cimini, A., & Moresi, M. (2014). Beer clarification using ceramic tubular membranes. *Food and Bioprocess Technology,* 7, 2694–2710.

Cimini, A., & Moresi, M. (2015). Novel cold sterilization and stabilization process applied to a pale lager. *Journal of Food Engineering*, 145, 1–9.

Cimini, A., Marconi, O., Perretti, G., & Moresi, M. (2014). Novel procedure for lager beer clarification and stabilization using sequential enzymatic, centrifugal, regenerable PVPP and crossflow microfiltration processing. *Food and Bioprocess Technology,* 7, 3156–3165.

646 Colebrook, C. (1938-39). Turbulent flow in pipes, with particular reference to the
647 transition region between the smooth and rough pipe laws. *Journal of the*
648 *Institution of Civil Engineers*, London, 11, 133-156.
649 Crane Co. (1965) Flow of fluids through valves, fittings and pipe. Technical Paper No.
650 410, Chicago, Illinois, USA.
651 Doleček, P., & Cakl, J. (1998). Permeate flow in hexagonal 19-channel inorganic
652 membrane under filtration and backflush operating modes. *Journal of Membrane*
653 *Science*, 149, 171-179.
654 European Brewery Convention (2010). *Analytica-EBC*. Fachverlag Hans Carl,
655 Nürnberg, Germany.
656 Fillaudeau, L., Blanpain-Avet, P., & Daufin, G. (2006). Water, wastewater and waste
657 management in brewing industries. *Journal of Cleaner Production*, 14, 463-471.
658 Fillaudeau, L., Boissier, B., Moreau, A., Blanpain-Avet, P., Ermolaev, S., Jitariouk, N.,
659 & Gourdon, A. (2007). Investigation of rotating and vibrating filtration for
660 clarification of rough beer. *Journal of Food Engineering*, 80, 206-217.
661 Gan, Q., Field, R.W., Bird, M.R., England, R., Howell, J.A., McKechnie, M.T., &
662 O'Shaughnessy, C.L. (1997). Beer clarification by cross-flow microfiltration:
663 fouling mechanisms and flux enhancement. *Chemical Engineering Research and*
664 *Design*, 75A, 3-8.
665 Gan, Q., Howell, J.A., Field, R.W., England, R., Bird, M.R., & McKechinie, M.T.
666 (1999). Synergetic cleaning procedure for a ceramic membrane fouled by beer
667 microfiltration. *Journal of Membrane Science,* 155, 277-289.
668 Gan, Q., Howell, J.A., Field, R.W., England, R., Bird, M.R., O'Shaughnessy, C.L., &
669 McKechinie, M.T. (2001). Beer clarification by microfiltration: product quality

control and fractionation of particles and macromolecules. *Journal of Membrane Science*, 194 (2), 185-196.

Haaland, S. (1983) Simple and explicit formulas for the friction factor in turbulent flow. *Transactions of ASME, Journal of Fluids Engineering*, 103, 89-90.

Hyflux Membrane Manufacturing (2010) InoCep®: Ceramic hollow fibre membrane. p. 4 (http://www.hyfluxmembranes.com/pdf/brochures/inocep.pdf ) (last checked on May, 5th, 2015).

Kuiper, S., van Rijn, C., Nijdam, W., Raspe, O., van Wolferen, H., Krijnen, G., & Elwenspoek, M. (2002). Filtration of lager beer with microsieves: flux, permeate haze and in-line microscope observations. *Journal of Membrane Science*, 196, 159-170.

Mellis, R., Gill, W.N., Belfort, G. (1993). Fluid dynamics in a tubular membrane: theory and experiment. *Chemical Engineering Communications*, 122, 103-125.

Montgomery, D.C. (2005). *Design and Analysis of Experiments*. 6th Edn, John Wiley & Sons, Inc., USA, pp. 247-248.

Munson-McGee, S.H. (2002). An approximate analytical solution for the fluid dynamics of laminar flow in a porous tube. *Journal of Membrane Science*, 197, 223-230.

Noordman, T.R., Peet, C., Iverson, W., Broens, L., & van Hoof, S. (2001). Cross-flow filtration for clarification of lager beer: economic reality. *Master Brewers Association of Americas Technical Quarterly*, 38(4), 207-10.

Pal, S., Ambastha, S., Ghosh, T. B., De, S., DasGupta, S. (2008). Optical evaluation of deposition thickness and measurement of permeate flux enhancement of simulated

693 fruit juice in presence of turbulence promoters. *Journal of Membrane Science*,
694 315, 58-66.
695 Pall Corporation (2007). Data sheet PIMEMBRAEN: Pall® Membralox® ceramic
696 membranes and modules.
697 (http://www.pall.com/pdfs/Microelectronics/PIMEMBRAEN.pdf) (last checked
698 on May, 5th, 2015).
699 Sondhi, R., & Bhave, R. (2001). Role of backpulsing in fouling minimization in
700 crossflow filtration with ceramic membranes. *Journal of Membrane Science*, 186,
701 41-52.
702 Toledo, R. T.(2007) *Fundamentals of Food Process Engineering*. 3rd Edn, Springer
703 Science+Business Media, LLC, New York., pp. 199.
704 Vassilieff, C.S. (1994). An elliptic filtration variation on Poiseuille-type laminar
705 solutions of Navier-Stokes equations. *Journal of Membrane Science*, 91, 153-161.
706 Yazdanshenas, M., Soltanieh, M., Tabatabaei Nejad, S. A. R., Fillaudeau, L. (2010).
707 Cross-flow microfiltration of rough non-alcoholic beer and diluted malt extract
708 with tubular ceramic membranes: Investigation of fouling mechanisms. *Journal of*
709 *Membrane Science*, 362, 306–316.
710

**Table 1**

Specific water permeation rate ($\alpha_W$) together with its corresponding coefficient of determination ($r^2$) and number of observations (N), as determined by using the least squares method, for the ceramic hollow-fiber membrane module (CHFMM) as received or used for a time interval of 6 months with different number of open channels.

| **CHFMM Status** | **Channel no.** | **N** | **$\alpha_W$ [g $s^{-1}$ $bar^{-1}$]** | **$r^2$** |
|---|---|---|---|---|
| As received | 40 | 17 | 25.2 ± 0.6 | 0.992 |
| Used | 40 | 25 | 18.9 ± 0.6 | 0.976 |
| Used | 4 | 7 | 3.34 ± 0.06 | 0.998 |

**Table 2**

Mean and standard deviation of the main characteristics (pH; density, ρ; viscosity, η; turbidity at 20 °C, $H_{20°C}$, and 0 °C, $H_{0°C}$; total phenolic content, TP, color, C; β-glucans, BG; real extract, RE; original extract, OE; alcohol content, A) of the rough pale lager as collected from the brewery maturation tank (RB), as PVPP-stabilized and diluted with water as recommended by the *Birra Peroni* brewmaster (F), and as permeated (P) during the batch validation CFMF tests carried out under constant transmembrane pressure difference (3.68 bar), crossflow velocity (6 m $s^{-1}$), temperature (10.0±0.5 °C), and periodic $CO_2$ back-flushing. All determinations were triplicated.

| **Pale lager sample** | **pH** [-] | **ρ** [kg $m^{-3}$] | **η** [mPa s] | **$H_{20°C}$** [EBC] | **$H_{0°C}$** [EBC] | **TP** [mg $L^{-1}$] | **C** [EBC] | **BG** [mg $L^{-1}$] | **RE** [°Plato] | **OE** [°Plato] | **A** [% v/v] |
|---|---|---|---|---|---|---|---|---|---|---|---|
| RB | 4.30± 0.01 | 1012 ± 1 | 1.433 ± 0.01 | 12.2 ± 0.7 | 58.3±1.5 | 152±5 | 16.1 ± 0.5 | 13 ± 1 | 5.2 ± 0.04 | 17.7 ± 0.04 | 6.75 ± 0.02 |
| F | 4.30±0.01 | 1008 ± 1 | 1.42 ± 0.01 | 1.16 ± 0.02 | 1.77 ± 0.08 | 89±2 | 7.7 ± 0.5 | 9 ± 2 | 3.9 ± 0.04 | 13.2 ± 0.01 | 5.00 ± 0.02 |
| P | 4.20± 0.01 | 1007 ± 1 | 1.38 ± 0.02 | 0.21 ± 0.01 | 0.44 ± 0.06 | 88±1 | 7.5 ± 0.5 | 9 ± 2 | 3.5 ± 0.03 | 13.0 ± 0.06 | 5.03 ± 0.02 |

**Table 3**

Main experimental and calculated results of the total recycle CFMF tests using the 0.8-μm ceramic four hollow-fiber membrane module under different crossflow velocities ($v_S$) and transmembrane pressure differences (TMP): pressure at the input ($P_{in}$) and output ($P_{out}$) sections of the membrane module, experimental ($\Delta P_{exp}$) and theoretical ($\Delta P_{teo}$) pressure drops due to friction over the membrane module; the mean value and standard deviation of the quasi-steady-state permeation flux (J*) with the number of observations (N); retentate ($Q_R$), permeate ($Q_P$) and feed ($Q_F$) volumetric flow rates; axial feed ($Re_F$) and wall ($Re_W$) Reynolds numbers; Fanning friction factor (f); and theoretical pump power ($N_P$).

| **Parameter** | **Value** | | | | | | | | | | | | | | | | | | | | | **Unit** |
|---|---|---|---|---|---|---|---|---|---|---|---|---|---|---|---|---|---|---|---|---|---|---|
| $v_S$ | 1.5 | 1.5 | 1.5 | 1.5 | 2.0 | 2.0 | 2.0 | 2.0 | 2.5 | 2.5 | 2.5 | 2.5 | 4.0 | 4.0 | 4.0 | 4.0 | 6.0 | 6.0 | 6.0 | 6.0 | 6.0 | 6.0 | [m/s] |
| $P_{in}$ | 2.00 | 3.00 | 4.00 | 5.00 | 2.00 | 3.01 | 4.00 | 5.00 | 2.00 | 3.05 | 4.05 | 5.02 | 2.20 | 3.02 | 4.03 | 5.02 | 2.02 | 2.40 | 3.03 | 4.05 | 4.43 | 5.00 | [bar] |
| $P_{out}$ | 1.92 | 2.93 | 3.92 | 4.9 | 1.85 | 2.89 | 3.87 | 4.88 | 1.75 | 2.80 | 3.83 | 4.84 | 2.02 | 2.58 | 3.60 | 4.60 | 1.15 | 1.45 | 2.15 | 3.15 | 3.52 | 4.12 | [bar] |
| $\Delta P_{exp}$ | 0.08 | 0.08 | 0.08 | 0.10 | 0.15 | 0.12 | 0.13 | 0.12 | 0.25 | 0.25 | 0.22 | 0.18 | 0.18 | 0.44 | 0.43 | 0.42 | 0.87 | 0.95 | 0.88 | 0.90 | 0.91 | 0.88 | [bar] |
| TMP | 0.96 | 1.96 | 2.96 | 3.95 | 0.93 | 1.95 | 2.94 | 3.94 | 0.88 | 1.93 | 2.94 | 3.93 | 1.11 | 1.80 | 2.82 | 3.81 | 0.59 | 0.93 | 1.59 | 2.60 | 2.98 | 3.56 | [bar] |
| J* | 30±1 | 46±2 | 41±2 | 49±4 | 35±1 | 45±2 | 46±1 | 53±1 | 30±1 | 57±1 | 70±2 | 76±1 | 50±1 | 96±2 | 112±1 | 129±1 | 31±1 | 80±1 | 97±1 | 127±1 | 137±2 | 173±7 | [L $m^{-2}$ $h^{-1}$] |
| N | 4 | 4 | 4 | 3 | 4 | 4 | 4 | 4 | 4 | 4 | 4 | 4 | 4 | 10 | 4 | 4 | 4 | 4 | 4 | 4 | 4 | 12 | - |
| $Q_R$ | 152.7 | 152.7 | 152.7 | 152.7 | 203.6 | 203.6 | 203.6 | 203.6 | 254.5 | 254.5 | 254.5 | 254.5 | 407.2 | 407.2 | 407.2 | 407.2 | 610.7 | 610.7 | 610.7 | 610.7 | 610.7 | 610.7 | [L $h^{-1}$] |
| $Q_P$ | 0.21 | 0.33 | 0.29 | 0.35 | 0.25 | 0.32 | 0.33 | 0.38 | 0.21 | 0.40 | 0.50 | 0.54 | 0.36 | 0.68 | 0.80 | 0.92 | 0.22 | 0.57 | 0.69 | 0.90 | 0.97 | 1.23 | [L $h^{-1}$] |
| $Q_F$ | 152.9 | 153.0 | 153.0 | 153.0 | 203.8 | 203.9 | 203.9 | 204.0 | 254.7 | 254.9 | 255.0 | 255.0 | 407.5 | 407.8 | 407.9 | 408.1 | 610.9 | 611.3 | 611.4 | 611.6 | 611.7 | 612.0 | [L $h^{-1}$] |
| $Re_F$ | 3191 | 3191 | 3191 | 3191 | 4255 | 4255 | 4255 | 4255 | 5319 | 5319 | 5319 | 5319 | 8510 | 8510 | 8510 | 8510 | 12765 | 12765 | 12765 | 12765 | 12765 | 12765 | [-] |
| $Re_W$ | 0.009 | 0.014 | 0.012 | 0.014 | 0.010 | 0.013 | 0.014 | 0.016 | 0.009 | 0.017 | 0.021 | 0.022 | 0.015 | 0.028 | 0.033 | 0.038 | 0.009 | 0.024 | 0.029 | 0.037 | 0.040 | 0.051 | [-] |
| f | 0.011 | 0.011 | 0.011 | 0.011 | 0.010 | 0.010 | 0.010 | 0.010 | 0.010 | 0.010 | 0.010 | 0.010 | 0.008 | 0.008 | 0.008 | 0.008 | 0.007 | 0.007 | 0.007 | 0.007 | 0.007 | 0.007 | [-] |
| $\Delta P_D$ | 0.03 | 0.03 | 0.03 | 0.03 | 0.06 | 0.06 | 0.06 | 0.06 | 0.08 | 0.08 | 0.08 | 0.08 | 0.17 | 0.17 | 0.17 | 0.17 | 0.35 | 0.35 | 0.35 | 0.35 | 0.35 | 0.35 | [bar] |
| $N_P$ | 4.4 | 8.6 | 12.9 | 17.1 | 5.9 | 11.6 | 17.3 | 22.9 | 7.7 | 15.1 | 22.1 | 29.0 | 14.9 | 24.8 | 36.2 | 47.4 | 23.3 | 30.1 | 40.5 | 58.0 | 64.5 | 74.1 | [W] |

**Figure 1**

Overall-(**a**) and front-(**b**) views of the 0.8-μm ceramic hollow-fiber membrane module used in this work and composed of 40 open channels together with its front-view after sealing 36 out of 40 channels with a silicone adhesive plug (**c**) and covering them with a stainless steel disk (**d**).

**1a)**

**1b)**

**1c)**

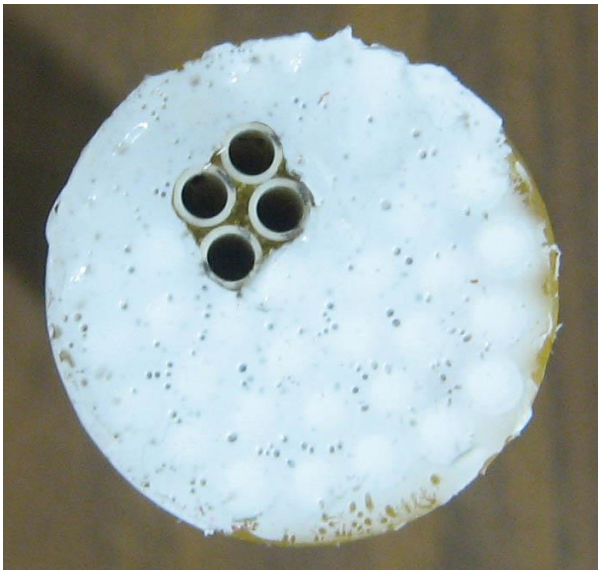

**1d)**

**Figure 2**

Effect of the transmembrane pressure difference (TMP) on the permeate mass flow rate ($Q_p$) for the ceramic 40 hollow-fiber membrane module, as received (closed symbols) or after 6-month using and cleaning (open symbols), and for partitioned four hollow-fiber membrane module (∗, ×), when setting the superficial velocity ($v_S$) at 0.5 ( ●, ○), 1.5 (■, □), 2.0 (△,×) or 6 (∗) m $s^{-1}$. Each broken line refers to the least squares regression equation, their corresponding slopes ($\alpha_W$) being reported in Table 1.

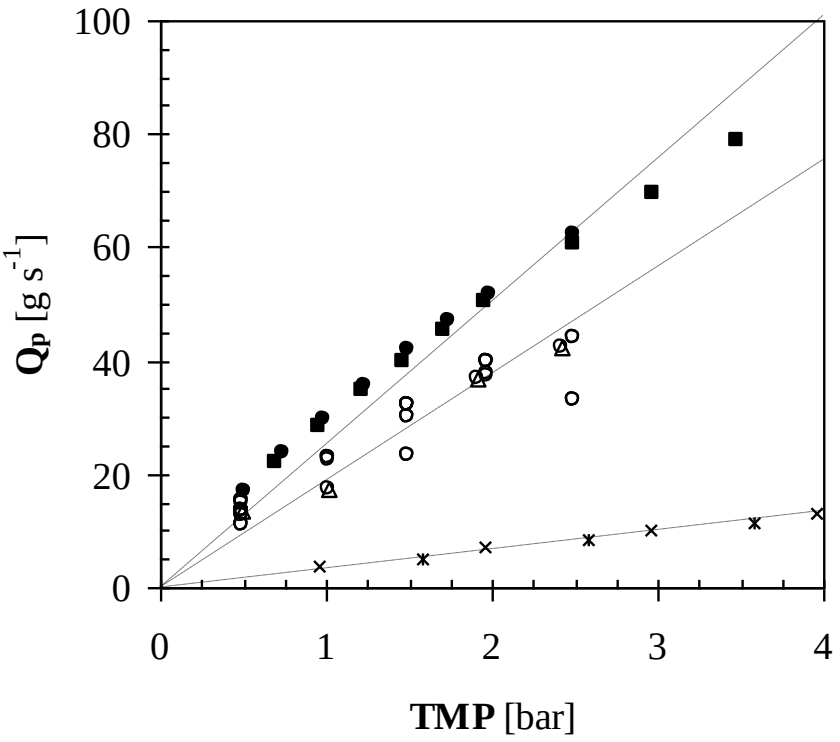

**Figure 3**

Time course of the overall membrane resistance ($R_T$) as resulting from a step by step increase in the transmembrane pressure difference (TMP) and crossflow velocity ($v_S$) when dealing with pre-centrifuged rough lager samples and operating with the 0.8-μm ceramic partitioned hollow-fiber membrane module at 10 °C and different $v_S$ values: ○, 1.5 m $s^{-1}$; △, 2.0 m $s^{-1}$; □, 2.5 m $s^{-1}$; ◇, 4.0 m $s^{-1}$; ∗, 6.0 m $s^{-1}$. For all characteristics of pre-centrifuged rough beer samples see Table 2. The broken line shows the intrinsic membrane resistance ($R_m$) of the membrane module used, while the bar errors for $R_T$ were ±10%.

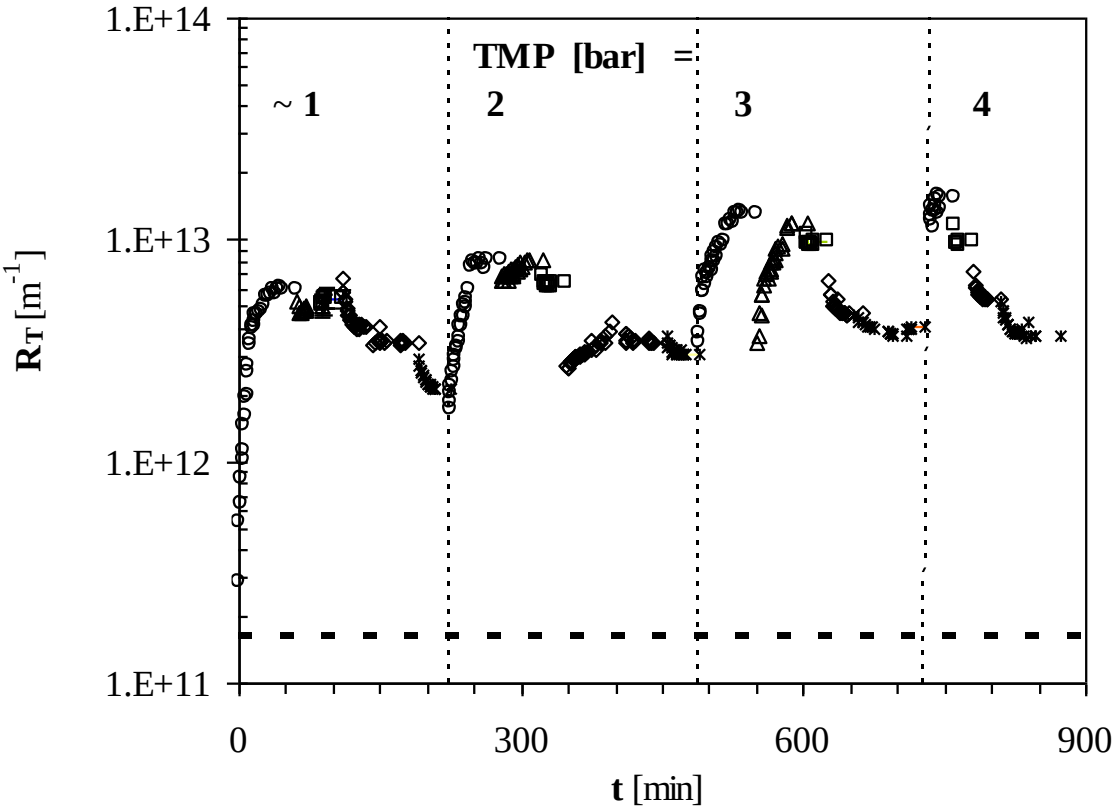

**Figure 4**

Effect of the transmembrane pressure difference (TMP) on the quasi-steady state permeation flux (J*) by setting the crossflow velocity ($v_S$) at 1.5 (○), 2.0 (△), 2.5 (□), 4 (◊) or 6 (∗) m $s^{-1}$. The continuous line illustrates the J* values calculated via Eq. (16), while the broken lines refer to loci of the upper and lower 95% confidence limits. The dash-dot lines refer to the least squares regression equations.

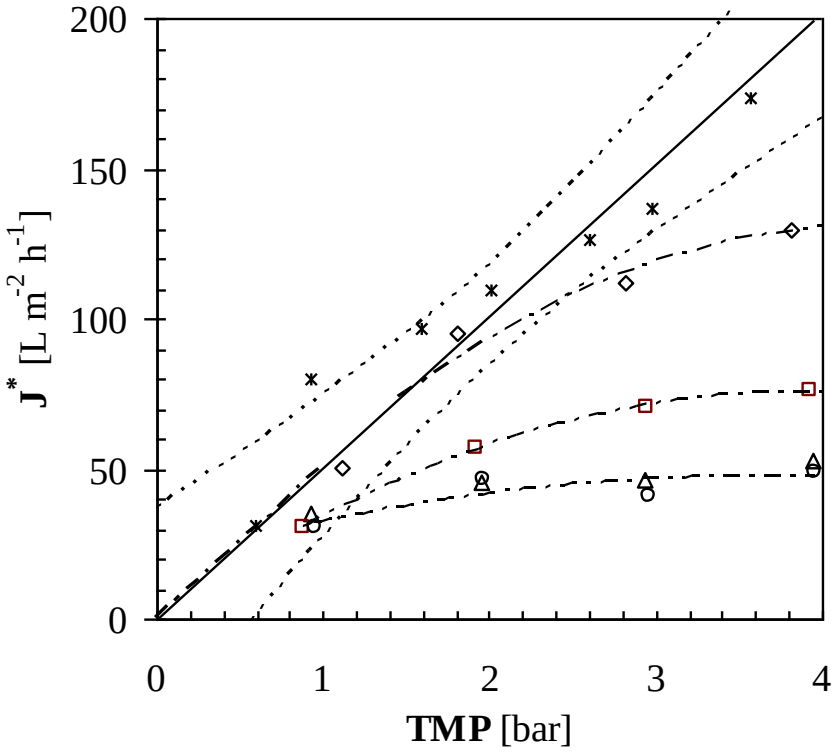

**Figure 5**

Relationship between the theoretical pump power need ($N_P$) and quasi-steady state permeation flux (J*) under different crossflow velocities ($v_S$): 1.5 (○), 2.0 (△), 2.5 (□), 4 (◊), or 6 (∗) m $s^{-1}$. The continuous line illustrates the J* values calculated via Eq. (22), while the broken lines refer to loci of the upper and lower 95% confidence limits.

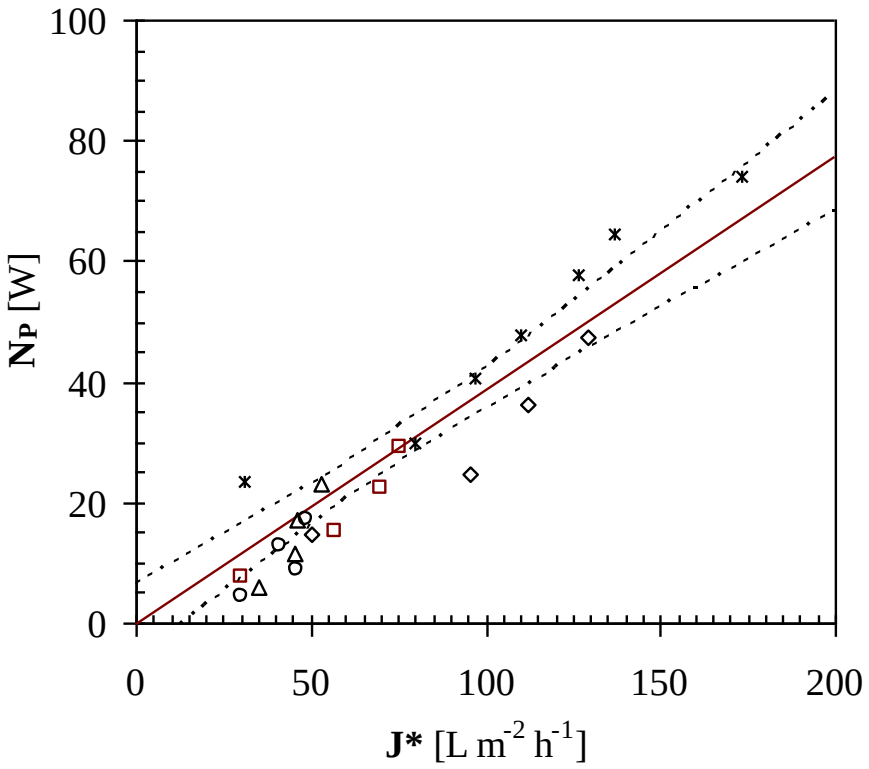

**Figure 6**

Time course of the permeation flux ($J_v$) of pre-centrifuges, PVPP-stabilized, and cartridge-filtered rough pale lager using the 0.8-μm ceramic hollow-fiber (○) or tubular (■) membrane module (as extracted from Cimini and Moresi, 2015) under the CFMF conditions given in the text and periodic $CO_2$ back-flushing. For all characteristics of the final pale lager permeate sample (P) see Table 2. The continuous or broken line represents the average permeation flux ($J_{v,av}$), as calculated using Eq. (3) and referred to the operation in the hollow-fiber or tubular membrane module, respectively. The average coefficient of variation for $J_v$ was about 10%.

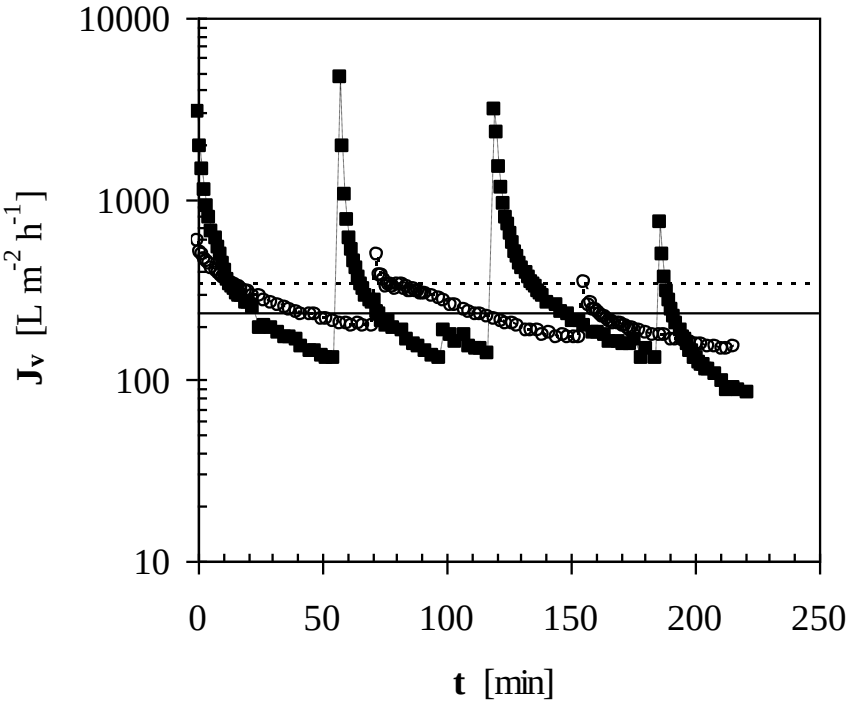

**Figure 7**

Time course of the permeation flux ($J_v$: ▲) of pre-centrifuges, PVPP-stabilized, and cartridge-filtered rough pale lager using the 0.8-μm ceramic four hollow-fiber membrane module at constant crossflow velocity (1.5 m $s^{-1}$) and temperature (10 °C) and feed input pressure ($P_{in}$) progressively increasing from 2 to 5 bar (continuous line) as soon as $J_v$ approached the quasi-steady state permeation flux. The broken line represents the average permeation flux ($J_{v,av}$), as calculated using Eq. (3). The average coefficient of variation for $J_v$ was about 10%.